Solvent effects in integrated reaction-separation process of liquid-phase hydrogenation of furfural to furfuryl alcohol over CuAl$_2$O$_4$ catalysts

Sutarat Thongratkaew [a], Sirapassorn Kiatphuengporn [a], Anchalee Junkaew [a], Sanchai Kuboon [a], Narong Chanlek [b], Anusorn Seubsai [c], Bunyarat Rungtaweevoranit [a], Kajornsak Faungnawakij [a,*]

[a] National Nanotechnology Center (NANOTEC), National Science and Technology Development Agency (NSTDA), Pathum Thani 12120, Thailand
[b] Synchrotron Light Research Institute, 111 University Avenue, Muang, Nakhon Ratchasima 30000, Thailand
[c] Research Network of NANOTEC–KU on NanoCatalysts and NanoMaterials for Sustainable Energy and Environment, Kasetsart University, Bangkok 10900, Thailand

ARTICLE INFO

ABSTRACT

Selective hydrogenation of furfural to furfuryl alcohol over CuAl$_2$O$_4$ catalysts is studied in a batch reactor using a range of solvents of varying chemical properties. We find that the reactions in branched alcohols provide higher furfuryl alcohol yields compared to linear alcohols. Besides, the reactions performed in nonane and decane provide excellent furfuryl alcohol yields of 96%. In situ FTIR analysis indicates that the carbonyl group of furfural is preferentially adsorbed leading to such high catalyst performance. Importantly, the efficient production of furfuryl alcohol in immiscible solvents minimizing downstream process is achieved in this integrative reaction-separation concept.

1. Introduction

Biomass has the potential to be a viable replacement for finite fossil fuels to manufacture a range of commodities and liquid fuels [1]. Among biomass-derived chemicals, furfural (FF) is listed as one of the most important platform chemicals which can be converted to several chemicals such as furfuryl alcohol (FFA), tetrahydrofurfuryl alcohol (THFA), 2-methyl furan (2-MF), tetrahydrofurfural (THFF) and 2-methyl tetrahydrofuran (2-MTHF) (Scheme S1) [2]. The synthetic versatility of FF stems from its structure which is composed of a carbonyl (C=O) fragment, a π-conjugated (C=C–C=C) moiety, and a five-membered ring structure enabling several chemical transformations. In this aspect, selective hydrogenation of the carbonyl moiety of FF to FFA is an important process that consumes >60% of the furfural produced to make fine chemicals, resins, lubricants, fragrances, dispersants, and plasticizers [3,4]. Industrially, FFA is manufactured both in liquid and gas phases [5]. While the reactions in the gas phase generally provide FFA in good yields, the reactions in the liquid phase offer additional control by using the property of solvents to tune reaction performance.

Several noble metal catalysts such as Ru [6], Pd [7], and Pt [8] have been reported as highly active catalysts while transition metal-based catalysts Cu, Co, Ni, Zr, Mg, Fe, Ce, and Zn have also been documented to show hydrogenation activity toward FF [9–12]. Particularly,

Cu catalysts show good selectivity for the hydrogenation of the carbonyl group of FF [13]. Depending on the local configurations of the Cu active sites in alcoholic solvents, the catalytic activity and selectivity can vary greatly (Table S1). We recently reported CuAl$_2$O$_4$ spinel as a low-cost and high-performance catalyst for the FF hydrogenation to FFA using isopropanol and water as a solvent mixture obtaining FFA with a remarkable yield of 94%. However, the effects of solvents in such a catalytic system remain unknown which could drastically affect the reaction efficiency. Previous studies on the solvent effects of FF hydrogenation to FFA generally agree that higher hydrogen donating ability and polarity of the solvents promote FF conversion; and secondary alcohols such as 2-propanol have been concluded as the optimal solvent [4,14,15]. However, the solvent studies are limited to some selected solvents prompting us to investigate the possibility of using other solvent systems to improve reaction efficiency [16].

Here, we comprehensively investigated the roles of solvents including protic solvents such as methanol, ethanol, 1-butanol, isopropanol, and 2-butanol; and aprotic solvents including pentane, hexanes, heptane, octane, nonane and decane for the hydrogenation of FF to FFA over CuAl$_2$O$_4$ spinel catalysts. Such an extensive list of solvents allowed us to correlate the properties of the solvents such as hydrogen donating ability and polarity with the FFA yields. For protic solvents, we found that the reactions in branched alcohols provide better FFA yields.

In contrast to previous reports, excellent FFA yields of 96% were obtained when nonane and decane were used as solvents despite the low hydrogen solubility in these solvents. The immiscibility of the FFA product is immiscible in these solvents facilitating the easy and rapid isolation of FFA by a simple extraction and the solvents can be reused in this integrated reaction-separation approach. Additionally, insights on the high selectivity of FFA production have been studied by in situ FTIR analysis of adsorbed FF on the catalyst.

2. Experimental

2.1. Materials

2-Propanol (99.5%), 2-butanol (99%), nonane (99%), decane (95%), isopropanol ($\geq$99.5%), furfural (99%), furfuryl alcohol (98%), copper nitrate hemi(pentahydrate) (98%), aluminum nitrate nonahydrate (98%) and citric acid (99.5%) were obtained from Sigma-Aldrich. Hexanes (99%), methanol (99.99%), and pentane (97%) were purchased from Fisher chemicals. Heptane (99%) was obtained from Quick. Octane (98%) and 1-butanol (99.9%) were purchased from RCI Labscan. Ethanol (99.9%) was obtained from DUKSAN.

2.2. Catalyst preparation

$CuAl_2O_4$ was prepared by a sol-gel combustion method. Specifically, copper nitrate hemi(pentahydrate) (11.87 g) was dissolved in deionized water (100 mL) and stirred at 60 °C until completely dissolved. Then, aluminum nitrate nonahydrate (38.28 g) was introduced to the copper nitrate hemi(pentahydrate) solution and the solution was stirred at 60 °C for 2 h. After that, citric acid (44.35 g) was added to the solution and stirred at 60 °C for 1 h. The solution was then heated to 100 °C while stirring until all the water was evaporated resulting in a gel-like substance. The temperature was then increased to 300 °C to initiate the combustion process, yielding a fine black powder. Finally, the solid product was calcined for 4 h at 900 °C in the air. [17].

2.3. Catalysts characterization

The phase of the catalyst was investigated by powder X-ray diffraction (PXRD, Bruker D8 ADVANCE) using Cu Kα radiation operated at 40 kV and 40 mA. The data was collected using a step size of 0.02° in the 2θ range of 20°–80°. The temperature-programmed reduction was used to investigate the reducibility of catalysts (TPR, Dynamic Flow Chemisorption Quantachrome Instruments). In each TPR experiment, the catalyst (0.2 g) was pretreated in a He flows (30 mL/min) at 150 °C for 1 h with a ramp rate of 5 °C/min. The catalyst was cooled to 60 °C under He flow (30 mL/min). Finally, the catalyst was performed using a TPR setup. The H_2 temperature-programmed reduction (TPR) experiment was carried out using 10% H_2/Ar in the temperature range of 45–800 °C at a ramp rate of 5 °C/min. Thermogravimetric Analysis (TGA, METTLER TOLEDO) experiments on spent catalysts were carried out under airflow at temperatures from room temperature to 900 °C at 10 °C/min to analyze the extent of catalyst coking.

2.4. Catalysis test

The Cu-based catalyst was tested for FF hydrogenation reaction in a stainless-steel batch reactor with a magnetic stirrer. The catalyst was activated immediately before each experiment by reducing it to 10% H_2/N_2 at 350 °C for 3 h. After the catalyst activation, 5 mL of FF in 25 mL of selected organic solvents and 0.5 g of the pre-reduced catalyst were added to the reactor. The reaction was carried out at 170 °C and an initial H_2 pressure of 20 bar. The autoclave was cooled to room

temperature using an ice-water bath after the reaction. The liquid phase product was collected and the solid catalyst was removed by centrifugation. Then the liquid samples were analyzed by gas chromatography (GC-2010, Shimadzu) with a flame ionization detector using a capillary column (DB-WAX, Agilent Technologies). The FF conversion, FFA yields, and isolated yields are calculated using the following equations:

$$\text{Conversion (\%)} = \left(\frac{\text{moles of FF consumed}}{\text{moles of FF initially charged}} \right) \times 100\% \qquad (1)$$

$$\text{Yield (\%)} = \left(\frac{\text{moles of FFA produced}}{\text{theoretical moles of FFA}} \right) \times 100\% \qquad (2)$$

For the isolation of FFA, the catalysis was conducted using decane as a solvent. After the reaction, the solid catalyst was removed by centrifugation. The liquid phase containing FFA and decane layers was separated by a separatory funnel and the amount of FFA was determined by an analytical balance.

2.5. In situ infrared spectroscopy of furfural adsorbed on $CuAl_2O_4$ catalyst

The adsorption of FF on the catalyst surface was investigated using a Nicolet iS50 infrared spectrometer (Thermo Scientific, Waltham, MA, USA) equipped with a mercury-cadmium-telluride (MCT) detector, a diffuse reflection attachment Praying Mantis™ and a high-temperature reaction cell. The catalyst sample was reduced to 350 °C for 3 h in the reaction cell with 10% H_2/Ar (30 mL/min) and then cooled down to 30 °C. The cell was purged with Ar (30 mL/min) for 1 h to remove physisorbed H_2. Then, FF (40 μL) was added to the catalyst dropwise using a microsyringe and the time counter was started. The spectrum was recorded at 30–150 °C until all the physisorbed species were removed [18].

3. Results and discussion

3.1. The textural and chemical property of the Cu-based catalysts

The physical properties of the catalyst were studied by PXRD analysis (Fig. 1(a)). The fresh $CuAl_2O_4$ shows the diffraction peaks at 19.0°, 31.3°, 36.9°, 44.8°, 49.1°, 55.7°, 59.4°, 65.3°, 74.2°, 77.4°, and 78.5° which can be indexed to the cubic structure of the $CuAl_2O_4$ spinel phase (JCPDS 01–071-0966). After the reduction in H_2 at 350 °C, the peaks belonging to the $CuAl_2O_4$ spinel phase are broadened suggesting the reduction in crystallite size of the spinel phase. In addition, we observed the appearance of the peaks at 43.3°, 50.5°, and 74.2° (JCPDS 00–001-1242) which is attributed to the partial reduction of $CuAl_2O_4$ to Cu.

The H_2-TPR measurements were conducted to investigate the reduction characteristics of the catalyst (Fig. 1(b)). Three peaks were observed in the H_2-TPR profile: i) 260–300 °C, ii) 500–600 °C and iii) 630–750 °C. The first reduction peak was assigned to the reduction of Cu^{2+} in the $CuAl_2O_4$ to metallic Cu on the catalyst surface [19]. The peaks found at higher temperatures were attributed to the reduction of bulk CuO or metal oxide composite of $CuAl_2O_4$ [20].

The electronic state of Cu species in the fresh and reduced $CuAl_2O_4$ was probed by X-ray photoelectron spectroscopy (XPS). Fig. 1(c) shows XPS spectra in the Cu $2p_{3/2}$ region of the fresh and reduced $CuAl_2O_4$ catalysts. In the fresh catalyst, the primary peak located at 933.5 eV was observed corresponding to Cu^{2+} species. The satellite peaks of Cu^{2+} species were also noticed at 943.0 eV further confirming the presence of Cu^{2+} in the fresh catalyst. In situ, XPS measurements after the reduction process at 350 °C indicate mixed-valence Cu including Cu^0 and Cu^{2+} as evidenced by peaks appearing at 932.8 and 933.5 eV, respectively [21,22].
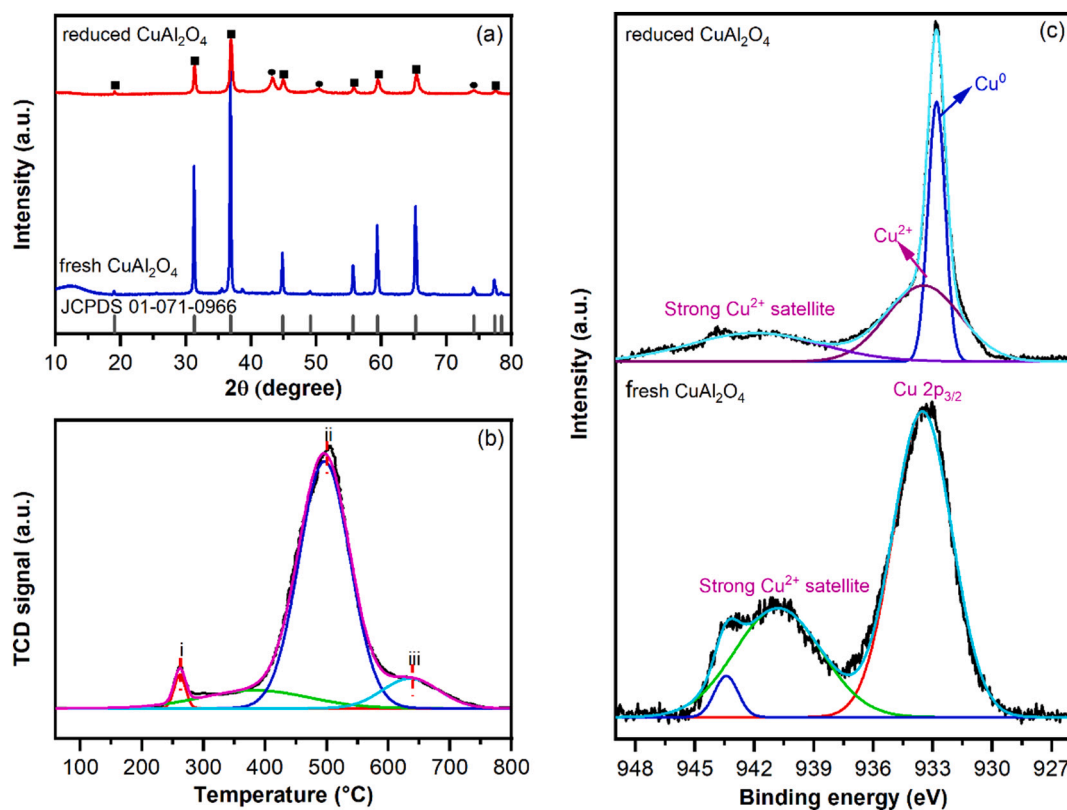
Fig. 1. (a) PXRD patterns of fresh and reduced CuAl$_2$O$_4$. ■ CuAl$_2$O$_4$ spinel ● Cu^0, (b) The H$_2$-TPR profile, and (C) XPS in the Cu 2p$_{3/2}$ region of the CuAl$_2$O$_4$ catalyst before and after the in-situ reduction.

3.2. The catalytic activity of Cu-based catalysts in furfural hydrogenation

Next, we studied the effects of organic solvents for FF hydrogenation at 170 °C and 20 bar of H$_2$. We selected two classes of organic solvents including alcohols and alkanes to understand the effects of the hydrogen donor ability of alcohol and the effects of biphasic systems.

3.2.1. Effects of alcohol solvents

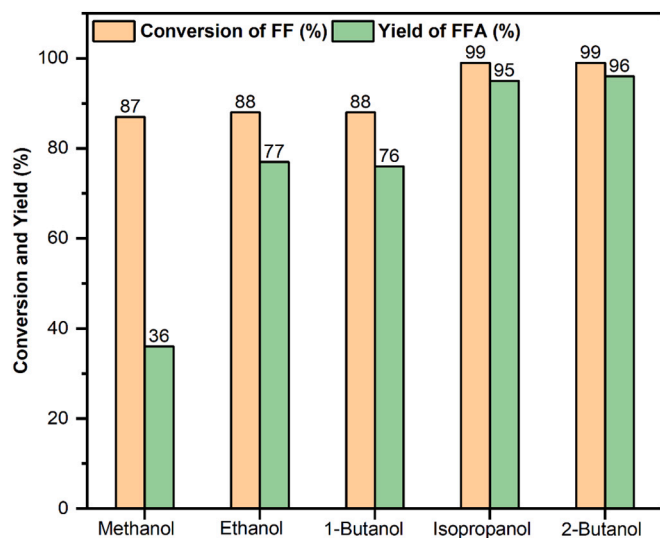Alcohol solvents are typically used in the hydrogenation of FF

Fig. 2. Effects of alcohol solvents on FF hydrogenation over the reduced CuAl$_2$O$_4$ catalyst. Reaction conditions: 0.5 g of reduced CuAl$_2$O$_4$, 2 mL of FF, 25 mL of solvent, 170 °C, 20 bar H$_2$, and 5 h.

because of their ability to generate hydrogen in situ via the catalytic transfer hydrogenation route and the solubility of FF in alcohol solvents [23,24]. We thus investigated such effects on the reduced CuAl$_2$O$_4$ catalyst by using a range of alcohol solvents including linear alcohols: methanol, ethanol, and 1-butanol; and branched alcohols: isopropanol and 2-butanol (Fig. 2). The highest FFA yield of 96% was obtained from the reaction using 2-butanol as a solvent followed by isopropanol (95%), ethanol (77%), 1-butanol (76%), and methanol (36%). To understand this trend, we first focus on the correlation with hydrogen donation ability. Such property has been reported to inversely correlate with the reduction potential of the alcohol ($\Delta_f H^\circ$) [25]. The reduction potential of alcohols decreases in the order of: methanol (130.1 kJ/mol) > > ethanol (85.4 kJ/mol) > 1-butanol (79.7 kJ/mol) > isopropanol (70.0 kJ/mol) ≈ 2-butanol (69.3 kJ/mol) [25,26]. Such a trend on the hydrogen donation property of alcohols is remarkably close to the FFA yields observed. Another factor that could affect the FFA yield is the solvent polarity which could be mapped with the π* value. The plot between FFA yields and π* values does not display any correlation (Fig. S1) suggesting that polarity is not the main factor in this catalytic system.

3.2.2. Effects of alkane solvents

Alkane solvents have not been widely used in the hydrogenation of FF which is likely due to the limited solubility of H$_2$ and FF in these solvents. Despite this, we previously found that the reduced CuAl$_2$O$_4$ catalyst has excellent H$_2$ sorption ability which could overcome the H$_2$ solubility issue. Accordingly, we performed the catalytic tests in solvents including pentane, hexanes, heptane, octane, nonane, and decane. There are several benefits of performing the reaction in these solvents. First, FF is sparingly soluble while FFA is insoluble in these solvents. During the reaction, FF will be reduced in the alkane phase to FFA where FFA is segregated from the alkane phase and thereby shifting the reaction equilibria toward FFA providing better FFA yield. Second, since FFA is separated from alkane solvent, FFA can be conveniently isolated from
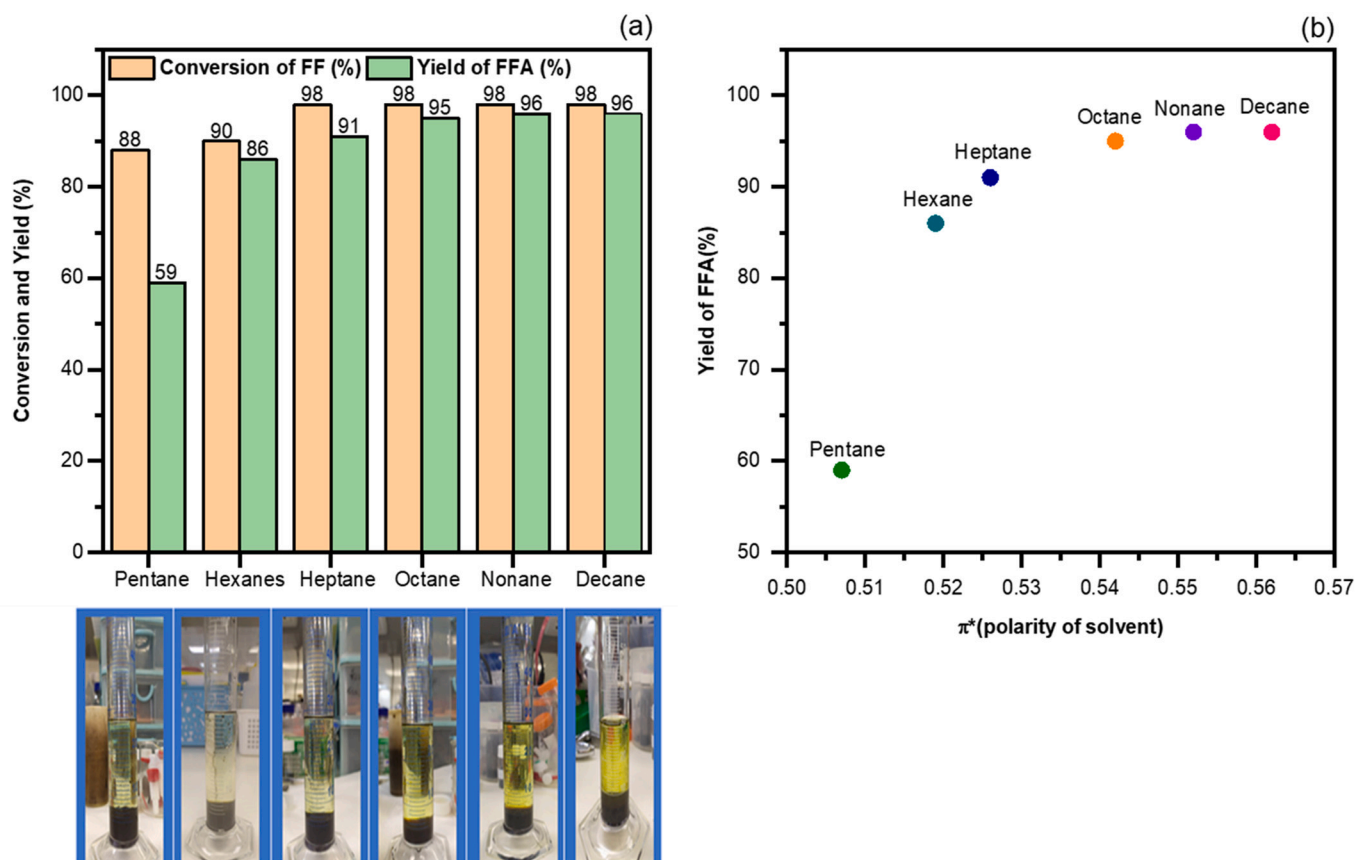
Fig. 3. (a) Effects of alkane solvents on the catalytic activity of reduced $CuAl_2O_4$ catalyst. Pictures of the reactions after the catalysis showing phase separation of FFA (bottom layer) from the alkane solvents (top layer). Reaction conditions: 0.5 g of reduced $CuAl_2O_4$, 2 mL of FF, 25 mL of solvent, 170 °C, 20 bar H_2 and 5 h. (b) The FFA yields from the reactions using different solvents were plotted against the polarity of the respective solvents.

the solvent by a simple liquid-liquid separation without additional solvent. Third, phase-separated alkane solvents can then be reused for the next reaction.

From the catalytic test, we found that the FF conversions in the alkane solvents were high in the range of 88–98% (Fig. 3(a)). However, we found that the FFA yields increase monotonically as a function of solvent chain length in the order: pentane (59%) < hexane (86%) < heptane (91%) < octane (95%) ~ nonane (96%) ~ decane (96%). We ruled out hydrogen solubility as the main factor because H_2 solubility is similarly low in these solvents [27]. Another parameter that could influence the FFA yield is the polarity of the solvent. As such, FFA yields from the reactions using different solvents were plotted against the polarity of the respective solvents (Fig. 3b) [28]. From this graph, we observe a correlation between higher solvent polarity providing higher FFA yield. Therefore, increasing polarity of the longer alkyl chain of the solvents is likely the main factor for this observed trend [29,30]. After the reactions, the spent catalysts were characterized by PXRD where the patterns are comparable to the pattern of the reduced $CuAl_2O_4$ (Fig. S2).

As expected, the reactions carried out in these alkane solvents yield two separated phases including alkane and FFA (Fig. 3). Remarkably, the FFA phase obtained from the reactions in octane, nonane, and decane contains only FFA without any typical reaction by-products such as 2-MF, THF, THFF, and 2-MTHF as indicated by the GC analysis [31]. This catalytic system thus provides excellent FFA yield with ease of FFA isolation.

To demonstrate the ease of product isolation, after the catalysis using decane as a solvent, the FFA layer was separated from the decane layer using a separatory funnel. The isolated FFA yield was 50–60%. This value is lower than the value determined by GC analysis because FFA is lost during the catalyst removal and the product transfer in such a small-

scale reaction while the mixture of spent catalyst and furfural product needs additional separation step.

We then assessed the recyclability of the $CuAl_2O_4$ catalyst under optimal conditions using decane as a solvent (Fig. S4). After each run, the catalyst was isolated by centrifugation, washed several times with decane, dried at 105 °C overnight, and reduced to 10% H_2/N_2 at 350 °C for 3 h. The FF conversions and FFA yields decrease gradually in the second and third cycles. The reduction in catalyst performance is attributable to the deposition of coke formation on the catalyst as indicated by TGA analysis (Fig. S5). Distinct weight loss between 100 and 600 °C was observed corresponding to the loss of solvent and carbon deposit on the catalyst. The catalyst was then regenerated in static air at 900 °C to remove the carbon deposit. After regeneration, the catalyst exhibited FF conversion of 89% and FFA yield of 80% which is close to the performance obtained from the second cycle.

3.3. Infrared absorption spectroscopy of furfural adsorbed on reduced $CuAl_2O_4$ catalyst

To understand the origin of high catalytic selectivity toward FFA over reduced $CuAl_2O_4$, in situ diffuse reflectance infrared Fourier transform spectroscopy (DRIFTS) was performed (Fig. 4). At 150 °C, peaks located at 1723, 1703, 1693, 1679, and 1673 cm^{-1} were observed which can be assigned to the C=O stretch of furfural. Upon heating to 200 °C which is above the boiling point of furfural, the peaks appearing at 1693 and 1676 cm^{-1} remain which belongs to the C=O stretch of furfural chemisorbed on the catalyst η^1(O) configuration [32]. Such red-shift compared to the gas phase furfural (1720 cm^{-1}) indicates the activation of the C=O group. Notably, the IR bands of the furan skeleton (1569, 1475, and 1464 cm^{-1}) are similar to those of FF in the gas phase
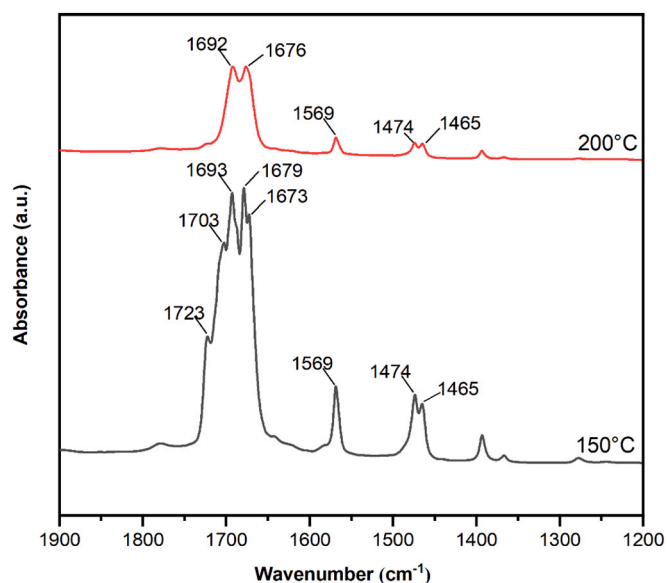
Fig. 4. In situ DRIFTS of adsorbed furfural on reduced $CuAl_2O_4$ collected at 150 °C and 200 °C after pretreatment in H_2 at 350 °C for 3 h.

hinting that the furan group does not have significant interaction with the catalyst [33–35]. Overall, FF is adsorbed on the reduced $CuAl_2O_4$ catalyst with the C=O group alone interacting with the catalyst which could explain the selective hydrogenation of the carbonyl group of FF to produce FFA.

4. Conclusions

In this study, we studied the effects of solvents on the hydrogenation of furfural over $CuAl_2O_4$ catalysts. High FF conversions (maximum of 98%) and FFA yields (maximum of 95%) were achieved in the reactions using branched alcohols such as isopropanol and 2-butanol and long alkanes such as octane, nonane, and decane as solvents. We found that the main factor contributing to the high FFA yields is different for different solvent systems. For alcohol solvents, the hydrogen donating ability of alcohols has been identified as a key parameter. In contrast, for alkane solvents, the combination of the high H_2 sorption property of $CuAl_2O_4$ catalyst and high solvent polarity seems to play a key role in providing high FFA yields. The use of alkane solvent systems is advantageous for scale-up production since FFA spontaneously separates from the alkane solvents facilitating the FFA isolation process. From in situ DRIFTS of adsorbed FF, selective hydrogenation of the carbonyl group of FF was attained by the preferred adsorption of the carbonyl portion over the furan ring of FF on the catalyst surface.

CRediT authorship contribution statement

Sutarat Thongratkaew: Investigation, Data curation, Methodology, Writing – original draft. **Sirapassorn Kiatphuengporn:** Methodology. **Anchalee Junkaew:** Investigation. **Sanchai Kuboon:** Methodology, Investigation. **Narong Chanlek:** Methodology, Investigation. **Anusorn Seubsai:** Investigation. **Bunyarat Rungtaweevoranit:** Data curation, Methodology, Formal analysis, Supervision, Writing – original draft, Writing – review & editing. **Kajornsak Faungnawakij:** Conceptualization, Methodology, Validation, Supervision, Project administration, Funding acquisition, Writing – review & editing.

Declaration of Competing Interest

There are no conflicts to declare.

Appendix A. Supplementary data

Supplementary data to this article can be found online at https://doi.org/10.1016/j.catcom.2022.106468.

References

[1] B. Liu, Z. Zhang, Catalytic conversion of biomass into chemicals and fuels over magnetic catalysts, ACS Catal. 6 (2016) 326–338.

[2] J. Zhang, D. Wu, Aqueous phase catalytic hydrogenation of furfural to furfuryl alcohol over in-situ synthesized Cu–Zn/SiO2 catalysts, Mater. Chem. Phys. 260 (2021), 124152.

[3] K. Fulajtárova, T. Soták, M. Hronec, I. Vávra, E. Dobročka, M. Omastová, Aqueous phase hydrogenation of furfural to furfuryl alcohol over Pd–Cu catalysts, Appl. Catal. A Gen. 502 (2015) 78–85.

[4] Y. Deng, R. Gao, L. Lin, T. Liu, X.-D. Wen, S. Wang, D. Ma, Solvent tunes the selectivity of hydrogenation reaction over α-MoC catalyst, J. Am. Chem. Soc. 140 (2018) 14481–14489.

[5] G. Gómez Millán, H. Sixta, Towards the green synthesis of furfuryl alcohol in a one-pot system from xylose: a review, Catalysts 10 (2020) 1101.

[6] C. Ramirez-Barria, M. Isaacs, K. Wilson, A. Guerrero-Ruiz, I. Rodríguez-Ramos, Optimization of ruthenium based catalysts for the aqueous phase hydrogenation of furfural to furfuryl alcohol, Appl. Catal. A Gen. 563 (2018) 177–184.

[7] K. Salnikova, V. Matveeva, A. Bykov, G. Demidenko, I. Shkileva, E. Sulman, The liquid phase catalytic hydrogenation of the furfural to furfuryl alcohol, Chem. Eng. Trans. 70 (2018) 379–384.

[8] X. Chen, L. Zhang, B. Zhang, X. Guo, X. Mu, Highly selective hydrogenation of furfural to furfuryl alcohol over Pt nanoparticles supported on g-C3N4 nanosheets catalysts in water, Sci. Rep. 6 (2016) 28558.

[9] M.M. Villaverde, T.F. Garetto, A.J. Marchi, Liquid-phase transfer hydrogenation of furfural to furfuryl alcohol on Cu–Mg–Al catalysts, Catal. Commun. 58 (2015) 6–10.

[10] P. Weerachawanasak, P. Krawmanee, W. Inkamhaeng, F.J.C.S. Aires, T. Sooknoi, J. Panpranot, Development of bimetallic Ni-Cu/SiO2 catalysts for liquid phase selective hydrogenation of furfural to furfuryl alcohol, Catal. Commun. 149 (2021), 106221.

[11] C.P. Jiménez-Gómez, J.A. Cecilia, F.I. Franco-Duro, M. Pozo, R. Moreno-Tost, P. Maireles-Torres, Promotion effect of Ce or Zn oxides for improving furfuryl alcohol yield in the furfural hydrogenation using inexpensive Cu-based catalysts, Mol. Catalys. 455 (2018) 121–131.

[12] W. Tolek, K. Khruechao, B. Pongthawornsakun, O. Mekasuwandumrong, F.J.C. S. Aires, P. Weerachawanasak, J. Panpranot, Flame spray-synthesized Pt-Co/TiO2 catalysts for the selective hydrogenation of furfural to furfuryl alcohol, Catal. Commun. 149 (2021), 106246.

[13] M.M. Villaverde, N.M. Bertero, T.F. Garetto, A.J. Marchi, Selective liquid-phase hydrogenation of furfural to furfuryl alcohol over Cu-based catalysts, Catal. Today 213 (2013) 87–92.

[14] P. Jia, X. Lan, X. Li, T. Wang, Highly selective hydrogenation of furfural to cyclopentanone over a NiFe bimetallic catalyst in a methanol/water solution with a solvent effect, ACS Sustain. Chem. Eng. 7 (2019) 15221–15229.

[15] J. Zhang, K. Dong, W. Luo, H. Guan, Selective transfer hydrogenation of furfural into furfuryl alcohol on Zr-containing catalysts using lower alcohols as hydrogen donors, ACS Omega 3 (2018) 6206–6216.

[16] C.B.T.L. Lee, T.Y. Wu, A review on solvent systems for furfural production from lignocellulosic biomass, Renew. Sust. Energ. Rev. 137 (2021), 110172.

[17] S. Thongratkaew, C. Luadthong, S. Kiatphuengporn, P. Khemthong, P. Hirunsit, K. Faungnawakij, Cu-Al spinel-oxide catalysts for selective hydrogenation of furfural to furfuryl alcohol, Catal. Today 367 (2021) 177–188.

[18] Z. Wang, X. Wang, C. Zhang, M. Arai, L. Zhou, F. Zhao, Selective hydrogenation of furfural to furfuryl alcohol over Pd/TiH2 catalyst, Mol. Catalys. 508 (2021), 111599.

[19] B.K. Kwak, D.S. Park, Y.S. Yun, J. Yi, Preparation and characterization of nanocrystalline CuAl2O4 spinel catalysts by sol–gel method for the hydrogenolysis of glycerol, Catal. Commun. 24 (2012) 90–95.

[20] A.M. Bahmanpour, F. Héroguel, M. Kılıç, C.J. Baranowski, L. Artiglia, U. Röthlisberger, J.S. Luterbacher, O. Kröcher, Cu–Al spinel as a highly active and stable catalyst for the reverse water gas shift reaction, ACS Catal. 9 (2019) 6243–6251.

[21] Y. Xu, Z. Lin, Y. Zheng, J.P. Dacquin, S. Royer, H. Zhang, Mechanism and kinetics of catalytic ozonation for elimination of organic compounds with spinel-type CuAl2O4 and its precursor, Sci. Total Environ. 651 (2019) 2585–2596.

[22] J. Zhang, C. Shao, X. Li, J. Xin, S. Yang, Y. Liu, Electrospun CuAl 2 O 4 hollow nanofibers as visible light photocatalyst with enhanced activity and excellent stability under acid and alkali conditions, CrystEngComm 20 (2018) 312–322.

[23] X. Gao, S. Tian, Y. Jin, X. Wan, C. Zhou, R. Chen, Y. Dai, Y. Yang, Bimetallic PtFe-catalyzed selective hydrogenation of furfural to furfuryl alcohol: solvent effect of isopropanol and hydrogen activation, ACS Sustain. Chem. Eng. 8 (2020) 12722–12730.

[24] G. Singh, L. Singh, J. Gahtori, R.K. Gupta, C. Samanta, R. Bal, A. Bordoloi, Catalytic hydrogenation of furfural to furfuryl alcohol over chromium-free catalyst: enhanced selectivity in the presence of solvent, Mol. Catalys. 500 (2021) 111339.

[25] X. Tang, H. Chen, L. Hu, W. Hao, Y. Sun, X. Zeng, L. Lin, S. Liu, Conversion of biomass to γ-valerolactone by catalytic transfer hydrogenation of ethyl levulinate over metal hydroxides, Appl. Catal. B Environ. 147 (2014) 827–834.

[26] J. Van der Waal, P. Kunkeler, K. Tan, H. Van Bekkum, Zeolite titanium beta: a selective catalyst for the gas-phase Meerwein–Ponndorf–Verley, and Oppenauer reactions, J. Catal. 173 (1998) 74–83.

[27] G. Ivaniš, L.F. Žilnik, B. Likozar, M. Grilc, Hydrogen solubility in bio-based furfural and furfuryl alcohol at elevated temperatures and pressures relevant for hydrodeoxygenation, Fuel 290 (2021), 120021.

[28] J.C. Sierra, Solvent Effects Based on Pure Solvent Scales, Handbook of Solvents, ChemTec Publishing, 2001, pp. 583–616.

[29] W. Schuddeboom, S.A. Jonker, J.M. Warman, U. Leinhos, W. Kuehnle, K. A. Zachariasse, Excited-state dipole moments of dual fluorescent 4-(dialkylamino) benzonitriles: influence of alkyl chain length and effective solvent polarity, J. Phys. Chem. 96 (1992) 10809–10819.

[30] M. Ouyang, C. Zhuo, F. Cao, G. Pan, C. Lv, S. Yang, C. Li, C. Zhang, J. Sun, Y. Zhang, Organogelator based on long alkyl chain attached excimer precursor: two channels of TICT, highly efficient and switchable luminescence, Dyes Pigments 180 (2020), 108433.

[31] G. Giorgianni, S. Abate, G. Centi, S. Perathoner, S. van Beuzekom, S.-H. Soo-Tang, J.C. Van der Waal, Effect of the solvent in enhancing the selectivity to furan derivatives in the catalytic hydrogenation of furfural, ACS Sustain. Chem. Eng. 6 (2018) 16235–16247.

[32] S. Sitthisa, T. Sooknoi, Y. Ma, P.B. Balbuena, D.E. Resasco, Kinetics and mechanism of hydrogenation of furfural on Cu/SiO2 catalysts, J. Catal. 277 (2011) 1–13.

[33] Z. Tong, X. Li, J. Dong, R. Gao, Q. Deng, J. Wang, Z. Zeng, J.-J. Zou, S. Deng, Adsorption configuration-determined selective hydrogenative ring opening and ring rearrangement of furfural over metal phosphate, ACS Catal. 11 (2021) 6406–6415.

[34] N. Alonso-Fagúndez, M. Ojeda, R. Mariscal, J.L.G. Fierro, M.L. Granados, Gas phase oxidation of furfural to maleic anhydride on V2O5/γ-Al2O3 catalysts: reaction conditions to slow down the deactivation, J. Catal. 348 (2017) 265–275.

[35] G. Allen, H. Bernstein, Internal rotation: VIII. The infrared and raman spectra of furfural, Can. J. Chem. 33 (1955) 1055–1061.